Electronic Supplementary Material (ESI) for Nanoscale.

Supporting Information

Extremely elastic and conductive N-doped graphene sponge for monitoring human motions

Jingxia Huang [a, b], Xiaohong Liu [a,] , Zhigang Yang [a], Xianzhang Wu [a, b], Jinqing Wang [a,*], and Shengrong Yang [a]

Corresponding authors. Tel: +86-931-4968076; Fax: +86-931-4968019.

E-mail addresses: jqwang@licp.cas.cn (J. Q. Wang); xhliu@licp.cas.cn (X. H. Liu)

The phrase abbreviations:

Ethanediamine (EDA)

Polyvinyl pyrrolidone (PVP)

Graphene oxide (GO)

Nitrogen-containing graphene aerogel (NGA)

Nitrogen-doped graphene sponge (NGS)

Scanning electron microscope (SEM)

Polarizing microscope (POM)

X-ray photoelectron spectroscopy (XPS)

As shown in Fig. S1, the optical photographs of graphene sponges obtained from GO, EDA, and various concentration of PVP system exhibit the various features. Apparently, it was difficult to form the monolith with the integrity configuration once the concentration of PVP over 3 mg mL^{-1}. It is deduced that the sufficient PVP were adsorbed on both sides of GO sheets, thusly reduced greatly the interaction between GO, leading to the weak self-assembling of GO sheets. Moreover, the low solution fluidity caused by the high concentration of PVP prevent the assembly channel of solution is another effective reason.

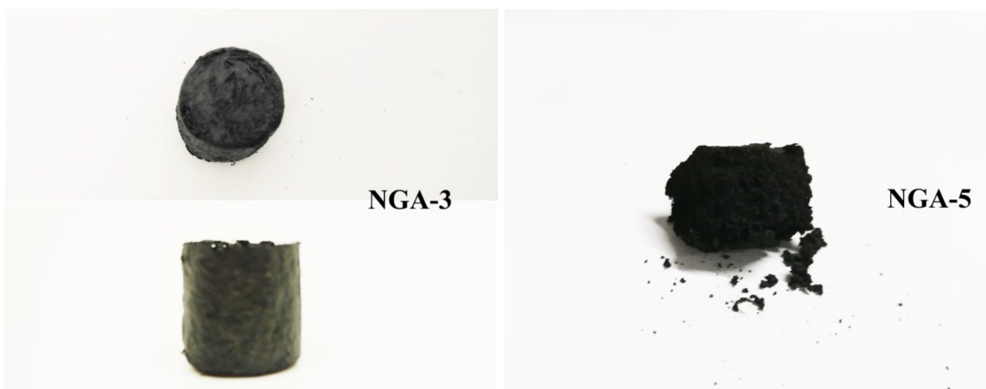

Fig. S1 Optical images of NGA-3 and NGA-5.

Table S1 Bulk density and electrical conductivity of the NGS with various concentration of PVP

Samples	Bulk density (mg cm^{-3})	Electrical conductance (S m^{-1})
NGA-0.5	17.19	0.33
NGS-0.5	7.75	0.67
NGS-1	8.44	0.82
NGS-2	9.17	1.05
NGS-3	9.31	1.40

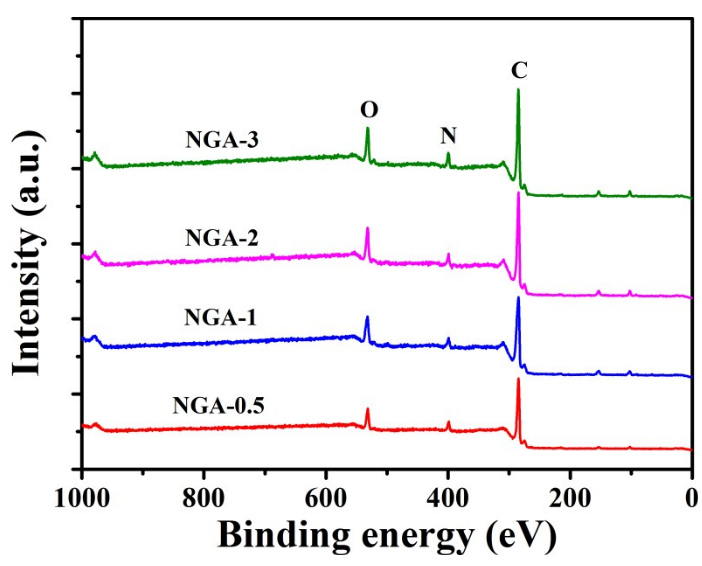

Fig. S2 XPS spectra of NGA obtained from different additive concentrations of PVP.

Table S2 Atomic composition of NGA from different additive concentrations of PVP determined by XPS analysis

Sample	C/O	N/C (%)	Atomic composition (at. %)		
			C	N	O
NGA-0.5	6.23	7.38	81.02	5.98	13.00
NGA-1	5.89	7.92	80.07	6.34	13.59
NGA-2	6.63	8.33	81.03	6.75	12.22
NGA-3	6.80	8.53	80.38	6.86	11.83

Table S3 Atomic composition of samples determined by XPS analysis

sample	C/O	N/C (%)	Atomic composition (at. %)		
			C	N	O
GO	2.64	--	72.51	--	27.49
NGA-3	6.82	8.31	80.38	6.86	11.83
NGS-3	10.94	3.43	88.83	3.05	8.12

Table S4 Nitrogen species deconvolution derived from XPS spectra

sample	N 1s (%)		
	Pyridinic N	Pyrrolic N	Quaternary N
NGA-3	--	56.13	43.87
NGS-3	15.73	11.35	72.92

*The N_P/N_Q atomic ratios were calculated according to the peak areas of N elements from XPS wide scans.

As shown in Fig. S3, the SEM images of graphene sponge from various systems exhibited that the graphene sponges have porous architecture. However, the morphology of graphene sponge from pure GO system exhibited the features of the absolutely disordered and scarcely porous structure (Fig. S3a). After the addition of EDA, the morphology showed the hierarchical porous structure and the graphene sheets are heavily stacked (Fig. S3b). It is noteworthy that the porous morphology of NGA obtained from GO, EDA, and PVP systems became gradually ordered and uniform with the concentration increases of PVP (Fig. S3c-f).

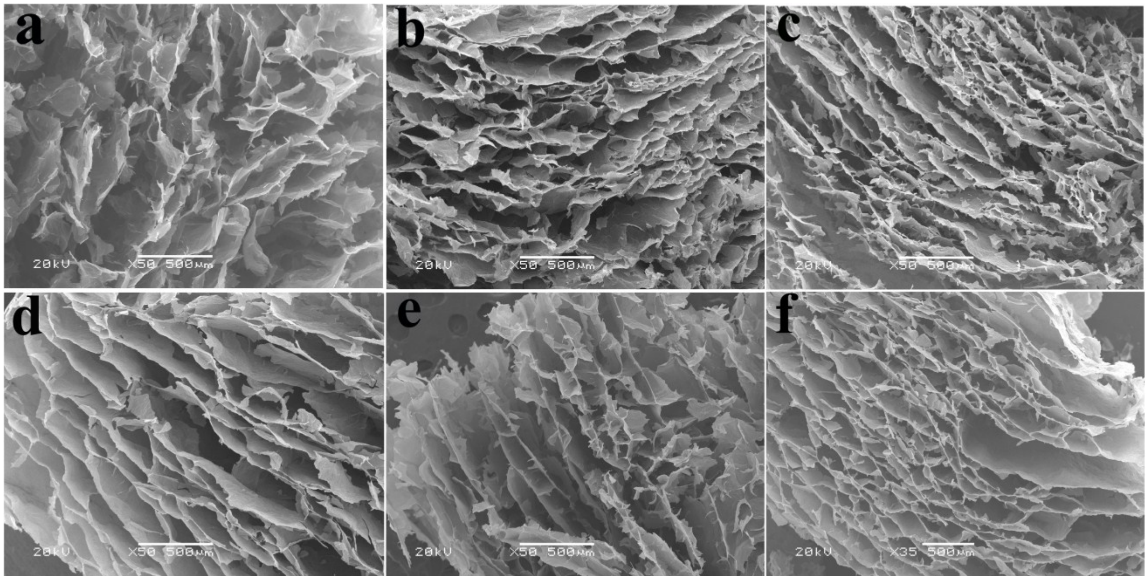

Fig. S3 SEM images of NGA from various system: (a) pure GO, (b-f) GO dispersion mixed with EDA and the different concentrations of PVP (0, 0.5, 1, 2, 3 mg/mL), respectively.

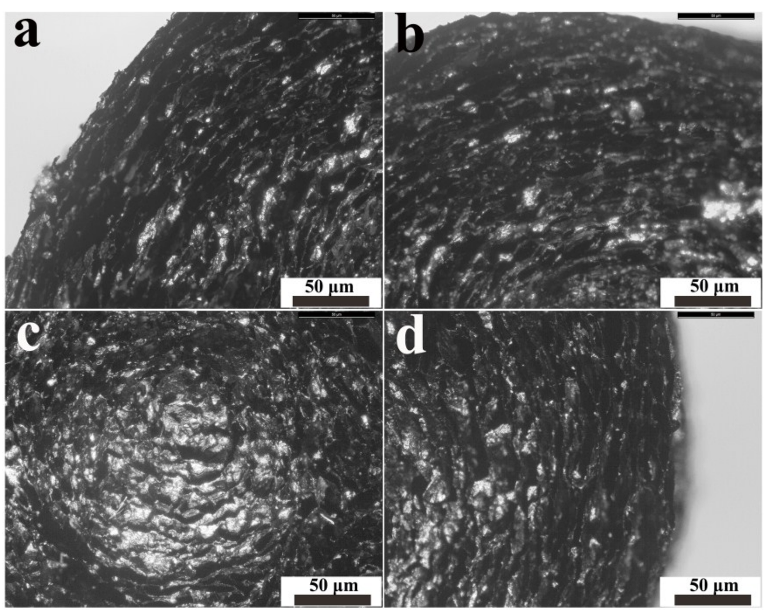

Fig. S4 The cross-section morphologies of NGA-3 by POM: (a) the top left corner, (b) right above of the center, (c) central area, and (d) the right of the center.

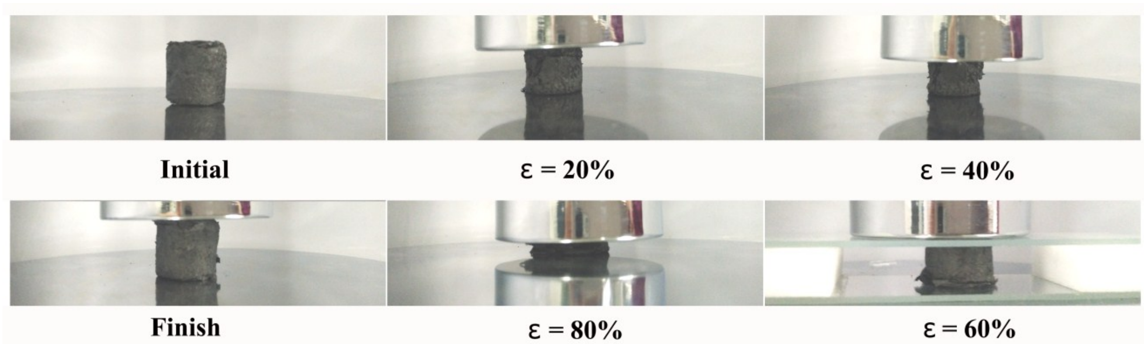

Fig. S5 Photographs of the NGS under the different strain amplitudes.

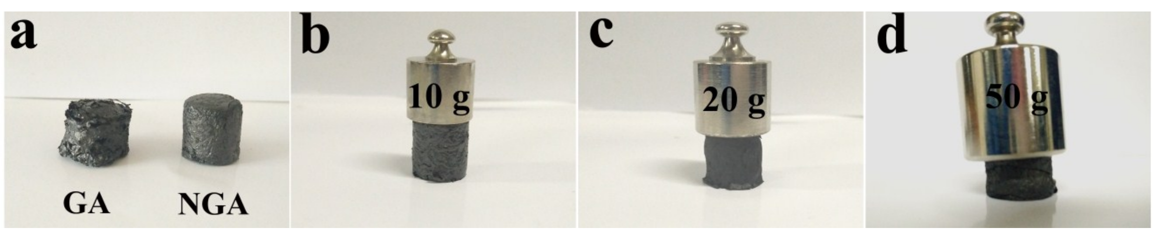

Fig. S6 (a) Photographs of graphene aerogel (GA) and NGA from pure GO system and the mixture of GO with PVP and EDA system, respectively. (b-d) Photographs of the loading tests, where 14 mg of NGA-3 supported 10, 20, and 50 g weight, respectively.

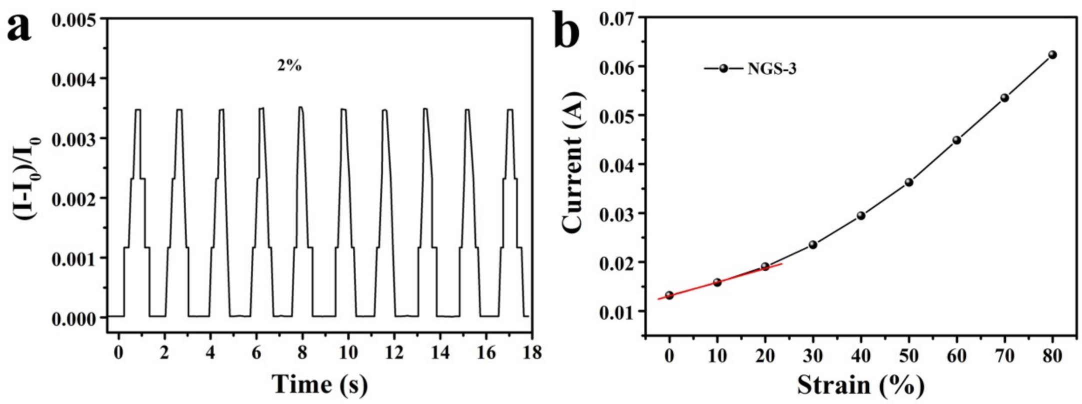

Fig. S7 (a) The sensing response of multiple cycles under 2% strain for NGS-3. (b) Variation of Current for NGS-3 with raising strains.

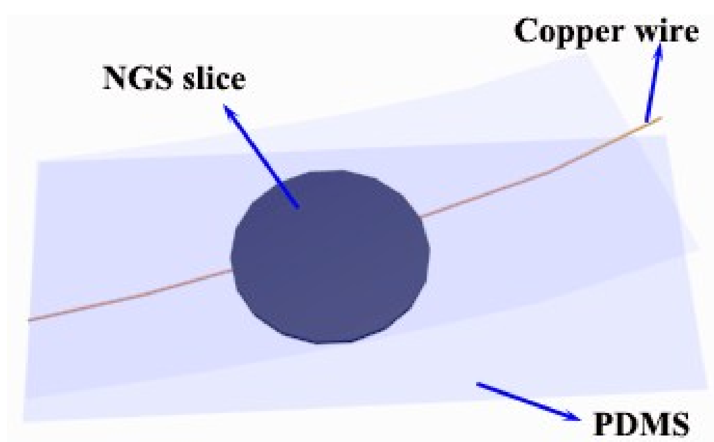

Fig. S8 Schematic of the wearable piezo-resistive sensor.

Table S5. Comparison of conductivity, compressibility, and durability for different foam materials

Sample	Density	Conductivity	Compressibility	Durability	Reference
SGA	3.72 mg cm^{-3}	--	99.5%	1000	1
GA	61 mg cm^{-3}	0.4 S m^{-1}	--	--	2
SGH	--	0.5 S m^{-1}	--	--	3
N-doped graphene aerogel	2.32 mg cm^{-3}	11.74 S m^{-1}	50%	10	4
MWCNT aerogel	4 mg cm^{3}	3.2 S m^{-1}	90%	1000	5
Graphene monolith	5.10 mg cm^{-3}	12 S m^{-1}	80%	10	6
EDA reduced graphene aerogel	6.9 mg cm^{-3}	--	70%	5	7
ULGA	10.9 mg cm^{-3}	--	90%	5	8
MWCNT-GA	2.52 mg cm^{-3}	320 Ω	80%	100	9
CNT aerogel	7.5 mg cm^{-3}		80%	10	10
CNF aerogel	--	--	80%	100	11
TRGO aerogel	29.1 mg cm^{-3}	--	60%	500	12
MGM	12.3 mg cm^{-3}	1.76 S m^{-1}	50%	10	13
GPA	27.2 mg cm^{-3}	1.0 S m^{-1}	--	--	14
UFA	22.4 mg cm^{-3}	~0.6 S m^{-1}	65%	1000	15
NGS	9.31 mg cm^{-3}	1.4 S m^{-1}	80%	>50	This work

Table S6. Comparison of sensitivity for different pressure sensors

Samples	Stress range	Sensitivity	Detection limit	Durability	Response time	References
MPS-GAs aerogel	0~1.5 kPa 7~8 kPa	0.22 kPa^{-1} 0.03 kPa^{-1}	--	100 cycles	--	16
rGO-PI foam	0~1.5 kPa 3.5~6.5 kPa	0.18 kP^{-1} 0.023kPa^{-1}	--	2000 cycles	--	17
ACC-PAA-alginate hydrogel	0~1 kPa	0.17 kPa^{-1}	--	100 cycles	--	18
RGO-PU sponge	0~2 kPa 2~10 kPa	0.26 kPa^{-1} 0.03 kPa^{-1}	9 Pa	10000 cycles	--	19
Coplanar-gate graphene-FET	0~40 kPa	0.12 kPa^{-1}	--	2500 cycles	--	20
CNT Ecoflex film	0~0.9 Mpa	0.00023 kPa^{-1}	--	12500 cycles	--	21
PDMS microstructure OFET	0~2 kPa 2~7 kPa	0.55 kPa^{-1} 0.15 kPa^{-1}	3 Pa	--	4 s	22
Au NW-PDMS paper	0~5 kPa	>1.14 kPa^{-1}	13 Pa	>50000 cycles	<17 ms	23
N-doped 3DG	0~10 kPa	4.5×10^{-2} kPa^{-1}	~15 Pa	--	0.7 s	24
GF	0~10 kPa	0.027 kPa^{-1}	--	--	80 ms	25
3D MX-rGO	0.4 kPa 22.56 kPa^{-1}	4.05 kPa^{-1} 22.56 kPa^{-1}	<10 Pa	10000 cycles	200 ms	26
SGA	0~0.5 kPa 0.5~1.5 kPa 1.5~2.5 kPa	-67.1 kPa^{-1} -8.6 kPa^{-1} -14.3 kPa^{-1}	<30 Pa	--	--	27
NGS	0~1kPa 1~3 kPa >3 kPa	0.15 kPa^{-1} 1.33 kPa^{-1} 0.51 kPa^{-1}	2% strain	3000 cycles	72.4 ms	This work

Table S7. Comparison of the linear sensing range for different materials-based strain sensors

Samples	sensing range	Detection limit	Durability	Response time	References
Fragmentized graphene foam-based strain sensor	< 20%	0.08%	10000 cycles	--	28
Fish-scale-like graphene-based strain sensor	20%~30%	<0.1%	>5000 cycles	--	29
ZnO nanowire/PSNF flexible films-based strain sensor	20%	1.5%	--	140 ms	30
Conductive polymer composite-based strain sensor	100%	--	--	50 ms	31
Nanofiber-based strain sensor	400%	0.5%	10000 cycles	5 ms	32
Graphite-based strain sensor	0.3%	~0.13%	1000 cycles	<110 ms	33
Ag NW Electronic fabric-based strain sensor	0~10%	--	10000 cycles	8 ms	34
SGA	--	~10%	--	--	27
N-doped 3DG	--	~0.2 % strain	--	0.7 s	24
NGS	~20%	2%	3000 cycles	72.4 ms	This work

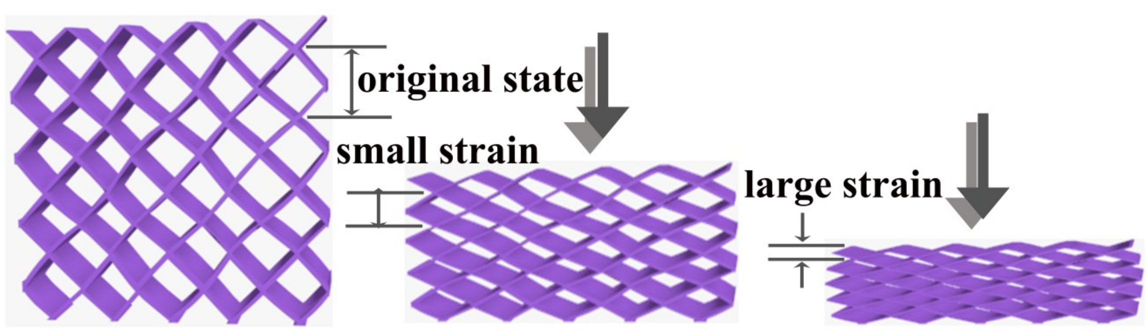

Fig. S9 Schematic illustration for the evolution of the conductive network in NGS during the compression test

Reference

1. J. L. Xiao, Y. Q. Tan, Y. H. Song, Q. Zheng, *Journal of Materials Chemistry A*, 2018, **6**, 9074-9080.

2. S. T. Nguyen, H. T. Nguyen, A. Rinaldi, N. P. V. Nguyue, Z. Fan, H. M. Duong, *Colloid and Surfaces A: Physicochemical and Engineering Aspects*, 2012, **414**(20), 352-358.

3. X. X. Xu, K. X. Sheng, C. Li, G. Q. Shi, *ACS Nano*, 2010, **4**(7), 4324-4330.

4. I. K. Moon, S. Yoon, K.-Y. Chun, J. W. Oh, *Advanced Functional Materials*, 2015, **25**, 6976-6984.

5. J. H. Zou, J. H. Liu, A. S. Karakoit, A. Kumar, D. Joung, Q. Li, S. I. Khondaker, S. Seal, L. Zhai, *ACS Nano,* 2010, **4**, 7293–7302.

6. L. Qiu, J. Z. Liu, L. Y. S. Chang, Y. Z. Wu, D. Li, *Nature Communications*, 2012, **3**, 1241.

7. J. H. Li, J. Y. Li, H. Meng, S. Y. Xie, B. W. Zhang, L. F. Li, H. J. Ma, J. Y. Zhang, M. Yu, *Journal of Materials Chemistry A*, 2014, **2**, 2934-2941.

8. H. Hu, Z. B. Zhao, W. B. Wan, Y. Gogotsi, J. S. Qiu, *Adv. Mater.*, 2013, **25**, 2219-2223.

9. L. Gao, F. Wang, W. W. Zhan, Y. Wang, G. Sui, X. P. Yang, *Chemistry Communications*, 2017, **53**, 521-524.

10. X. C. Gui, J. Q. Wei, K. L. Wang, A. Y. Cao, H. W. Zhu, Y. Jia, Q. K. Shu, D. H. Wu, *Advanced Materials*, 2010, **22**,617-621.

11. H. W. Liang, Q. F. Guan, L. F. Chen, Z. Zhu, W. J. Zhang, S. H. Yu, *Angewandte Chemie International Edition*, 2012, **51**, 5101-5105.

12. J. L. Xiao, J. F. Zhang, W. Y. Lv, Y. H. Song, Q. Zhang, *Carbon*, 2017, **123**, 354-363.

13. Y. Li, J. Chen, L. Huang, C. Li, J. D. Hong and G. Shi, *Advanced Materials*, 2014, **26**, 4789-4793.

14. G. Tang, Z.-G. Jiang, X. Li, H.-B. Zhang, A. Dasari and Z.-Z. Yu, *Carbon*, 2014, **77**, 592-599.

15. H. Sun, Z. Xu and C. Gao, *Advanced Materials*, 2013, **25**, 2554-2560.

16. P. Zhang, L. Lv, Z. Cheng, Y. Liang, Q. Zhou, Y. Zhao and L. Qu, *Chemistry-An Asian Journal*, 2016, **11**, 1071-1075.

17. Y. Qin, Q. Peng, Y. Ding, Z. Lin, C. Wang, Y. Li, F. Xu, J. Li, Y. Yuan, X. He, Y. Li, *ACS Nano*, 2015, **9**, 8933-8941.

18. Z. Lei, Q. Wang, S. Sun, W. Zhu and P. Wu, *Advanced Materials*, 2017, **29,** 1700321.

19. H. B. Yao, J. Ge, C. F. Wang, X. Wang, W. Hu, Z. J. Zheng, Y. Ni and S. H. Yu, *Advanced Materials*, 2013, **25**, 6692-6698.

20. Q. Sun, D. H. Kim, S. S. Park, N. Y. Lee, Y. Zhang, J. H. Lee, K. Cho and J. H. Cho, *Advanced Materials*, 2014, **26**, 4735-4740.

21. D. J. Lipomi, M. Vosgueritchian, B. C. Tee, S. L. Hellstrom, J. A. Lee, C. H. Fox and Z. Bao, *Nature Nanotechnology*, 2011, **6**, 788-792.

22. S. C. Mannsfeld, B. C. Tee, R. M. Stoltenberg, C. V. Chen, S. Barman, B. V. Muir, A.

N. Sokolov, C. Reese and Z. Bao, *Nature Materials*, 2010, **9**, 859-864.

23. S. Gong, W. Schwalb, Y. W. Wang, Y. Chen, Y. Tang, J. Si, B. Shirinzadeh, W. L. Cheng, *Nature Communications*, 2014, **5**, 3132.
24. M. A. S. M. Haniff, S. M. Hafiz, N. M. Huang, S. A. Rahman, K. A. A. Wahid, M. I. Syono, I. A. Azid, *ACS Applied Materials & Interfaces*, 2017, **9**, 15192-15201.
25. J. Yang, X. Li, X. Lu, W. Bao, R. Chen, doi:10.1109/jsen.2018.2855691, IEEE Sensors Journal.
26. Y. N. Ma, Y. Yue, H. Zhang, F. Cheng, W. Q. Zhao, J. Y. Rao, S. J. Luo, J. Wang, X. L. Jiang, Z. T. Liu, N. S. Liu, Y. H. Guo, *ACS Nano*, 2018, **12**, 3209-3216.
27. J. L. Xiao, Y. Q. Tan, Y. H. Song, Q. Zheng, *Journal of Materials Chemistry A*, 2018, **6**, 9074-9080.
28. Y. R. Jeong, H. Park, S. W. Jin, S. Y. Hong, S. S. Lee, J. S. Ha, *Advanced Functional Materials*, 2015, **25**, 4228-4236.
29. Q. Liu, J. Chen, Y. R. Li, G. Q. Shi, *ACS Nano*, 2016, **10**, 7901-7906.
30. X. Xiao, L. Y. Yuan, J. W. Zhong, T. P. Ding, Y. Liu, Z. X. Cai, Y. G. Rong, H. W. Han, J. Zhou, Z. L. Wang, *Advanced Materials*, 2011, **23**, 5440-5444.
31. T. Wang, Y. Zhang, Q. C. Liu, C. Wen, X. R. Wang, L. J. Pan, B. X. Xu, H. X. Xu, *Advanced Functional Materials*, 2018, **28**, 1705551.
32. K. Qi, J. X. He, H. B. Wang, Y. M. Zhou, X. L. You, N. Nan, W. L. Shao, L. D. Wang, B. Ding, S. Z. Cui, *ACS Applied Materials & Interfaces*, 2017, **9**, 42951-42960.

33. X. Q. Liao, Q. L. Liao, X. Q. Yan, Q. J. Liang, H. N. Si, M. H. Li, H. L. Wu, S. Y. Cao, Y. Zhang, *Advanced Functional Materials*, 2015, **25**, 2395-2401.

34. J. Ge, L. Sun, F. R. Zhang, Y. Zhang, L. A. Shi, H. Y. Zhao, H. W. Zhu, H. L. Jiang, S. H. Yu, *Advanced Materials*, 2016, **28**, 722-728.